Bachelor Thesis

Investigating the Gribov Problem through the Faddeev-Popov Operator Eigenspectrum in SU(2)

Nicole Oberth

Supervisor: Univ.-Prof. Dipl.-Phys. Dr.rer.nat. Axel Maas

Department of Physics
University of Graz

2023

Contents

1 Introduction and Theory

1.1 Objective

The following thesis aims to examine the eigenspectrum of the Faddeev-Popov operator in non-Abelian $SU(2)$ Yang-Mills theories using analytical methods. Specifically, the Gribov problem will be explored, the objective being to find negative eigenvalues. As a gauge, the Landau gauge is chosen and the potential is given in the form of a simple potential well, described via the hyperbolic tangent function.

1.2 Gauge Theories

Classical electrodynamics

Historically, the first encounter with gauge symmetries was in classical electrodynamics, and serves as a reasonable introduction. The scalar potential V and the vector potential $\vec{A}$ are introduced and defined via the measurable electric field E and the magnetic flux density $\vec{B}$:

$$\vec{B} = \nabla \times \vec{A}$$

$$\vec{E} = -\nabla V - \frac{\partial \vec{A}}{\partial t}$$

It is clear that the potentials are not uniquely defined, meaning that they can be transformed without changing the corresponding fields. The transformations of the fields under which the fields are invariant are known as gauge transformations.[1]

$$\begin{aligned} \vec{A}' &= \vec{A} + \nabla\lambda \\ V' &= V - \frac{\partial \lambda}{\partial t} \end{aligned} \tag{1}$$

In this case, $\lambda(\vec{r}, t)$ is an arbitrary scalar function.

This results in a large number of additional degrees of freedom. To reduce these, a gauge can be enforced. In electrodynamics, the Lorentz gauge is convenient as it provides both scalar and vector potentials with simple expressions.

$$\nabla \cdot \vec{A} = -\mu_0 \epsilon_0 \frac{\partial V}{\partial t} \tag{2}$$

Formalism using scalar fields

When switching to the field description of particles, the particle position in space $x(t)$ is replaced by a scalar field $\phi(x_\mu)$, dependent on the four-vector $x_\mu = (x, y, z, t)$ with the Lagrangian

$$\mathscr{L} = (\partial_\mu \phi)(\partial^\mu \phi^*) - m^2 \phi^* \phi \tag{3}$$

3 is invariant under the gauge transformation (and the corresponding complex conjugate):

$$\phi \to e^{-i\Lambda} \phi \tag{4}$$

For local gauge invariance, $\Lambda(x^\mu)$ will be a function of the four-vector.

The transformation can be written as a rotation in the 2d plane, but is also unitary, showing that the symmetry group in electromagnetism is $SO(2) \approx U(1)$. Due to Noether's theorem, with this symmetry, there is a conserved current J^0 and a resulting conserved quantity, which is the electric charge Q in this case.[6]

Because $\Lambda(x^\mu)$ is dependent on x^μ, the derivatives in 3 contain extra terms. To maintain gauge invariance, a 4-potential A_μ is introduced in form of additions to the Lagrangian. It couples to the current J^μ and has the following gauge transformation:

$$A_\mu \rightarrow A_\mu + \frac{1}{e}\partial^\mu \Lambda \tag{5}$$

Here, e is the electric charge and represents a coupling constant. The curl of A_μ is also added into the Lagrangian - in electromagnetism, it represents the electromagnetic field tensor:

$$F_{\mu\nu} = \partial^\mu A_\nu - \partial_\nu A_\mu \tag{6}$$

As the derivative $\partial^\mu \phi$ transforms differently than ϕ, it is replaced with the covariant derivative D_μ to keep the invariance:

$$D_\mu \phi = (\partial^\mu + ieA_\mu)\phi \tag{7}$$

This leads to the complete Lagrangian of the electromagnetic field:

$$\mathscr{L}_{EM} = D_\mu \phi D^\mu \phi^* - m^2 \phi^* \phi - \frac{1}{4} F^{\mu\nu} F_{\mu\nu} \tag{8}$$

Yang-Mills theories

In gauge fields, the local gauge transformations under which the Lagrangian is invariant form a Lie group. While the electromagnetism example showed a relatively simple gauge group of $U(1)$, Yang-Mills fields can have symmetries in form of a variety of Lie groups (as long as they are compact and reductive) - the focus of this thesis is that of the $SU(2)$ group. It is isomorphic to the $SO(3)$ group and non-Abelian. This has several physical consequences, specifically the fact that it is self-interacting.[4][6]

The local gauge transformation under $SU(2)$ is the following:

$$\psi(x) \rightarrow \exp\left(i\Lambda^i(x)\frac{\sigma^i}{2}\right) \tag{9}$$

with $\Lambda^i(x)$ being arbitrary functions, and σ^i the Pauli matrices, the generators of the $SU(2)$ group (when multiplied with i):

$$\sigma_1 = \begin{pmatrix} 0 & 1 \\ 1 & 0 \end{pmatrix}, \sigma_2 = \begin{pmatrix} 0 & -i \\ i & 0 \end{pmatrix}, \sigma_3 = \begin{pmatrix} 1 & 0 \\ 0 & -1 \end{pmatrix}, \tag{10}$$

This transformation calls for a relevant covariant derivative:

$$D_\mu = \partial_\mu - igA^i_\mu \frac{\sigma^i}{2} \tag{11}$$

The gauge potential is now a vector with three components A^i_μ - so is the conserved current $\vec{J}_\mu$, which is called the source. 11 also gives rise to the coupling constant g. The generalization of the electromagnetic field tensor, the gauge field $F_{\mu\nu}$, is defined as follows:

$$F_{\mu\nu} = \partial_\mu A_\nu - \partial_\nu A_\mu - ig[A_\mu, A_\nu] \tag{12}$$

For Abelian groups, the result is clearly 6 - however, for the $SU(2)$ Yang Mills field, one refers to the commutation relation of the generators

$$[\sigma_i, \sigma_j] = 2i\epsilon_{ijk}\sigma_k \tag{13}$$

in order to get the gauge field:

$$F_{\mu\nu} = \partial_\mu A_\nu - \partial_\nu A_\mu - g\epsilon_{abc} A^b_\mu A^c_\nu \tag{14}$$

with the antisymmetric Levi-Civita tensor ϵ_{abc} acting as the $SU(2)$ structure constant f^{abc}. From these, the Yang-Mills Lagrangian can be constructed:

$$\mathscr{L}_{YM} = -\frac{1}{4}(F^i_{\mu\nu})^2 \tag{15}$$

The following fields are all $SU(2)$ Yang-Mills fields.

1.3 Faddeev-Popov Operator

Gauge fields are quantized via the path integral formulation and expressed with a generating functional

$$Z = \int \mathscr{D}A_\mu e^{i\int \mathscr{L}dx} = \int \mathscr{D}A_\mu e^{iS} \tag{16}$$

Because $\mathscr{L}$ and the action S are gauge invariant, the integral includes all possible potentials A_μ, resulting in a divergent integral. This is remedied by fixing a gauge and applying the Faddeev-Popov method. The gauge in question is the Landau gauge:

$$\partial_\mu A^\mu = 0 \tag{17}$$

The Landau gauge is a special case of the Lorentz gauge condition and is dependent on a parameter in the Feynman propagator, which will not be discussed in detail here. The gauge fixing is expressed as an additional term in the Lagrangian:

$$\mathscr{L} = -\frac{1}{4}F_{\mu\nu}F^{\mu\nu} - \frac{1}{2}(\partial_\mu A^\mu)^2 = \mathscr{L}_0 + \mathscr{L}_{GF} \tag{18}$$

$\mathscr{L}_0$ is given by 15.

The Faddeev-Popov method consists of inserting a "ghost term" into 16, further reducing the degrees of freedom.[4] This ghost term represents a field with no physical effect (in particle terms: a virtual particle), appearing as a "one" in the mathematical formalism. The following paragraphs provide a brief demonstration of the method, as well as a derivation of the corresponding Faddeev-Popov operator (derivation by [6]).

In the Yang-Mills field, the gauge transformation of A_μ^U can be written using the unitary matrices U:

$$A_\mu^U = UA_\mu U^\dagger - i(\partial_\mu U)U^\dagger$$
$$U = e^{i\Lambda^a(x)T^a}$$

with the infinitesimal form

$$A_\mu'^a = A_\mu^a + f^{abc}A_\mu^b\Lambda^c + \partial_\mu\Lambda^a$$

(for which T^i represent the generators and Λ^i the functions of the gauge transformation in the color index i).

In functional terms, the gauge condition (with the non-abelian color index a) is written as

$$F^a[A_\mu] = 0$$

meaning that for the Landau gauge, $F = \partial^\mu A_\mu$.

Now, a "one" can be inserted into the generating functional. Because the gauge transformation is described by the unitary matrix U and 1.3, it is possible to perform the path integral over U. A delta functional $\delta[F^a[A]]$ is used to cancel the integral and retain the "one":

$$\delta[F^a[A]] = \prod_{x^\mu,a} \delta(F^a[A(x^\mu)])$$

Now a functional $\Delta_F[A_\mu]$ is introduced, which, when multiplied with the integral, is equal to one:

$$\Delta_F[A_\mu]\int \mathscr{D}U\delta[F^a[A_\mu^U]] = 1$$

Inserting this into the generating functional and using $Z \sim \int \mathscr{D}\bar{A}_\mu e^{iS}\int \mathscr{D}\Lambda$ (the integral of the gauge term Λ can be separated out because of 1.3):

$$Z = \int \mathscr{D}A_\mu\Delta_F[A_\mu]\int \mathscr{D}U\delta[F^a[A_\mu^U]]e^{iS}$$

It can be shown that $\mathscr{D}A_\mu^U \equiv \mathscr{D}A_\mu$, and using 1.3 and the gauge invariance of $\Delta_F[A_\mu]$, the integral $\mathscr{D}U$ can be pulled out. It can be ignored as it is a multiplicative factor. Now,

$$Z = \int \mathscr{D}A_\mu \Delta_F[A_\mu]\delta[F^a[A_\mu]]e^{iS}$$

and the expression for $\Delta_F[A_\mu]$ is given by:

$$\Delta_F[A_\mu] = \det|\frac{\delta F}{\delta \Lambda}|_{F=0} \equiv \det\ M$$

with M being the Faddeev-Popov operator.

Using the equivalence $\int d\bar{\alpha}d\alpha e^{-\bar{\alpha}A\alpha} = \det\ A$, and multiplying i to M,

$$\det\ iM = \int \mathscr{D}\bar{\eta}\mathscr{D}\eta \exp\left(-i\int \bar{\eta}^a M_{ab}\eta^b dx\right) \tag{19}$$

This can be substituted into Z and gives rise to the Faddeev-Popov ghost term in the Lagrangian:

$$\mathscr{L}_{eff} = -\frac{1}{4}F_{\mu\nu}F^{\mu\nu} - \frac{1}{2}(\partial_\mu A^\mu)^2 - \bar{\eta}^a M_{ab}\eta^b = \mathscr{L}_0 + \mathscr{L}_{GF} + \mathscr{L}_{FPG}$$

with the ghost fields $\eta, \bar{\eta}$.

In Yang-Mills fields, 19 is used to define the definition of the Faddeev-Popov operator which is used in this thesis: [3]

$$M_{ab} = -\partial_\mu(\partial_\mu\delta^{ab} + gf^{abc}A_\mu^c) \tag{20}$$

1.4 Fiber bundles and Gribov ambiguity

To visualize the Gribov problem, it is helpful to describe gauge fixing with fiber bundles. A fiber bundle is a collection of topological spaces constructed of the following:
A space E (called the total space) is related to a base space M through a continuous surjective map $\pi : E \to M$, mapping elements of the total space onto the base space. A fiber F over a point $x \in M$ is described by the inverse $\pi^{-1}(x)$ of the map $\pi(x)$. The fibers are subspaces of E and are homeomorphic. When $\pi^{-1}(x) = F$ forms a topological space $\forall x$, the collection (E, π, M) forms a fiber bundle with the fiber F.[2][5] The following figure shows a simple sketch of a fiber bundle (E,π,M) with fiber F.

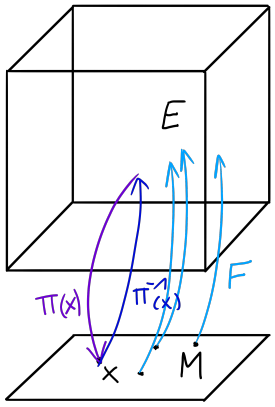

Figure 1: Sketch of the topological spaces that make up the fiber bundle, with total space E, base space M and fibers F, with the continuous maps $\pi(x)$ and $\pi^{-1}(x)$ for a point $x \in M$.

Fixing a gauge can be described as choosing a section of the fiber bundle, which means choosing a continuous map $\sigma : M \to E$ such that $\pi(\sigma(x)) = x$ for all points $x \in M$). Another description defines a fixed gauge as the intersection between the orbit of the gauge (here: the orbit of the $SU(2)$ group) and the fiber bundle at exactly one point. However, this is where the Gribov ambiguity arises. Gribov discovered that the orbits can globally intersect the fiber bundle more than once, or not at all. This especially tends to be the case for non-Abelian gauge theories and for gauges involving differentials (the Landau gauge 17 being one of these).[7]

Globally, this ambiguity cannot be controlled, but there is an attempt at a local remedy, in which the field configuration space is divided up into Gribov regions with boundaries known as Gribov horizons, which restrict the path integrals. The first Gribov region is bounded in all directions. Due to this, the fields in the path integral cannot be arbitrarily large. The Faddeev-Popov operator is positive in the first Gribov region, and in this thesis, the focus is to examine a potential for a spectrum in the Faddeev-Popov operator which contains negative eigenvalues, thereby going beyond the first Gribov region.[3][7]

2 Setting up the problem

The objective of the thesis is to calculate the eigenspectrum of the Faddeev-Popov operator M^{ab} (given in 20) for the color indices a, b, c:

$$M^{ab} = -\partial_\mu(\partial_\mu\delta^{ab} + gf^{abc}A^c_\mu)$$

The eigenspectrum will be calculated with the standard eigenvalue equation, with the eigenvalue λ and eigenfunctions ϕ^a, ϕ^b:

$$\lambda\phi^a = M^{ab}\phi^b \tag{21}$$

The Faddeev-Popov operator will be applied to a simple potential well, which should be at least a C^2 function, as it must be continuous and have both continuous first and second derivatives, as these are required in the operator definition. The chosen vector potential is therefore given by a hyperbolic tangent function, defined in Cartesian coordinates for the two-dimensional case:

$$A^c_\mu = \tanh ax^2$$

The width of the potential well can be controlled by the parameter a. This is set to 1, so the length is in units of a.

$$A^c_\mu = \tanh x^2 \tag{22}$$

Plugging this into 21 gives the eigenvalue equation to be solved:

$$\lambda\phi^a = -\sum_{b=1}^{3}(\partial^2\delta^{ab} + gf^{abc}A^c_\mu\partial_\mu)\phi^b \tag{23}$$

In the $SU(2)$ group, the structure constants f^{abc} are proportional to the Levi-Civita tensor (see the commutation relation 13):

$$f^{abc} = 2i\epsilon^{abc}$$

Now 23 can be split up depending on the color index, resulting in the cyclical and anticyclical differential equations for ϕ^1 and ϕ^2, respectively:

$$\lambda\phi^1 = -\partial^2\phi^1 - gf^{123}\partial_\mu A^3_\mu\phi^2 = -\partial^2\phi^1 - 2gi\tanh^2 x\partial_\mu\phi^2 \tag{24}$$

$$\lambda\phi^2 = -\partial^2\phi^2 - gf^{213}\partial_\mu A^3_\mu\phi^1 = -\partial^2\phi^2 + 2gi\tanh^2 x\partial_\mu\phi^1 \tag{25}$$

For $A^3 = A^a\delta^{a3}$ (color index 3 being the only non-zero entry for A^a_μ):

$$\lambda\phi^3 = -\partial^2\phi^3 \tag{26}$$

3 Analytical calculations

3.1 Vacuum solution

The differential equation in 26 does not involve the potential, and its solutions are therefore the vacuum solutions - it is to be expected that these are positive. Next, a few simplifications are used to make calculations easier, which will be used both for the vacuum equation and the coupled equations. One of these involves using the Euclidean metric instead of the Minkowski metric. This is made possible by performing a Wick rotation, replacing the time variable with an imaginary one ($t \to i\tau$), essentially working with an analytically continued theory with the Euclidean signature. It is assumed that the Wick rotation can be used, but it is not explicitly performed here, thus the time variable will remain t. The other simplification is the switch to polar coordinates, reducing to two Euclidean dimensions:

$$(\rho, \eta) \to \rho^2 = x^2 + t^2 \tag{27}$$

The differential operator ∂^2 becomes the Laplace operator Δ, which has the following definition in polar coordinates:

$$\Delta = \frac{\partial^2}{\partial\rho^2} + \frac{1}{\rho}\frac{\partial}{\partial\rho} + \frac{1}{\rho^2}\frac{\partial^2}{\partial\eta^2} \tag{28}$$

Plugging this into 26 results in a Helmholtz differential equation in polar coordinates, which can be solved via separation and yields the Bessel functions.[8] In Cartesian coordinates, the solutions take the form of plane waves.[3]

3.2 Coupled equations

The differential equations 24 and 25 are coupled. Analogous to 27, a switch to polar coordinates (ρ, η) is performed. Next, it is checked whether the coupled equations are separable for $\phi^i = \phi^i_\rho \phi^i_\eta$ (here for 24). Due to the coordinate transformation, ρ is multiplied to $\tanh^2(\rho)$.

$$\lambda \phi^1_\rho \phi^1_\eta = -\partial^2 \phi^1_\rho \phi^1_\eta - 2gi\rho \tanh^2(\rho) \partial_\mu \phi^2_\rho \phi^2_\eta \tag{29}$$

The differentials

$$\partial_\mu = \frac{1}{\rho}\partial_\rho \rho + \frac{1}{\rho}\partial_\eta$$

$$\partial^2 = \frac{1}{\rho}\partial_\rho \rho \partial_\rho + \frac{1}{\rho^2}\partial^2_\eta$$

are substituted into 29. Because the vector potential $A = A_\eta \hat{e}_\eta$ points in the η direction and the Landau gauge 17 holds, the η direction is projected outwards and the corresponding partial differential goes to zero. Thus, the differential ∂_μ only acts onto the ρ direction.

$$\lambda \phi^1_\rho \phi^1_\eta = -\frac{1}{\rho}\partial_\rho \phi^1_\rho \phi^1_\eta - \frac{1}{\rho^2}\partial^2_\eta \phi^1_\rho \phi^1_\eta - 2gi\rho \tanh^2(\rho) \cdot \frac{1}{\rho}\partial_\rho \rho \phi^2_\rho \phi^2_\eta$$

For the separation, the ρ and η components are brought to their respective sides:

$$\Rightarrow \lambda \phi^1_\rho \phi^1_\eta + \frac{\phi^1_\eta}{\rho}\partial_\rho \rho \partial_\rho \phi^1_\rho + \frac{1}{\rho^2}\partial^2_\eta \phi^1_\rho \phi^1_\eta = -\phi^2_\eta \cdot 2gi \tanh^2(\rho) \partial_\rho \rho \phi^2_\rho$$

$$\Rightarrow \frac{1}{\phi^2_\eta} \cdot [\phi^1_\eta \cdot (\lambda \phi^1_\rho + \frac{1}{\rho}\partial_\rho \rho \partial_\rho \phi^1_\rho) + \frac{\phi^1_\rho}{\rho^2} \cdot \partial^2_\eta \phi^1_\eta] = -2gi \tanh^2(\rho) \partial_\rho \rho \phi^2_\rho$$

$$\Rightarrow \frac{\phi^1_\eta}{\phi^2_\eta} \cdot (\lambda \rho^2 + \frac{\rho \partial_\rho \rho \partial_\rho \phi^1_\rho}{\phi^1_\rho}) + \frac{1}{\phi^2_\eta} \cdot \partial^2_\eta \phi^1_\eta = -\frac{1}{\phi^1_\rho} \cdot 2gi\rho^2 \tanh^2(\rho) \partial_\rho \rho \phi^2_\rho$$

Due to the periodicity of the angular component η, the following approach can be used for corresponding function ϕ_η:

$$\phi^i_\eta = a_i e^{i\omega_i \eta} + b_i e^{-i\tilde{\omega}_i \eta} \tag{30}$$

with the frequency

$$\omega_i = 2\pi n$$

Setting $\omega_1 = \omega_2$, the first term $\frac{\phi^1_\eta}{\phi^2_\eta} = 1$ and the equation can be separated:

$$\frac{1}{\phi^2_\eta} \cdot \partial^2_\eta \phi^1_\eta = -\lambda \rho^2 - \frac{\rho}{\phi^1_\rho}\partial_\rho \rho \partial_\rho \phi^1_\rho - \frac{1}{\phi^1_\rho} \cdot 2gi\rho^2 \tanh^2(\rho) \partial_\rho \rho \phi^2_\rho \tag{31}$$

Remark: Angular component

Using the solution 30 for the angular component of the equation 31, applying the differential ∂^2_η results in the following for the remaining term:

$$\frac{\partial^2_\eta \phi^\eta}{\phi^\eta} = \frac{-\omega^2(ae^{i\omega\eta} + be^{i\tilde{\omega}\eta})}{(ae^{i\omega\eta} + be^{i\tilde{\omega}\eta})} = -\omega^2$$

This results in the left side of the equation becoming a constant (renamed to κ).

$$-\omega^2 \equiv \kappa \tag{32}$$

3.3 Radial component

To solve for the radial ρ component, the equation 31 is rewritten to include the constant κ from 32:

$$(\kappa + \lambda\rho^2 + \rho\partial_\rho\rho\partial_\rho)\phi_\rho^1 = -2gi\rho^2 \tanh^2(\rho)\partial_\rho\rho\phi_\rho^2 \tag{33}$$

Behavior in limits

To get an idea of how the radial function component ϕ_ρ behaves at high and low ρ, ρ is sent to zero and infinite, and the corresponding, now simpler, differential equations are solved:

$\rho \to 0$

Sending ρ to zero, the $\tanh^2(\rho)$ vanishes. Using the product rule for $\rho\partial_\rho\rho\partial_\rho\phi^1$ and removing all terms with ρ^2 (as these vanish in comparison):

$$\kappa\phi^1 = -\lambda\rho^2\phi^1 - \rho\partial_\rho\phi^1 - \rho^2\partial_\rho^2\phi^1 - 2gi\rho^2 \tanh^2(\rho)\partial_\rho\rho\phi^2$$

Now the first-order differential equation is solved via separation of variables:

$$\Rightarrow \kappa\phi^1 = -\rho\partial_\rho\phi^1$$

$$\Rightarrow -\int \frac{1}{\phi} d\phi = \int \frac{\kappa}{\rho} d\rho$$

This results in symmetric ϕ^1 and ϕ^2 with two possible constants κ:

$$\phi_0^1 = \phi_0^2 \to \rho^{-\kappa}e^c = \begin{cases} 0 & \kappa \neq 0 \\ 1 & \kappa = 0 \end{cases} \tag{34}$$

$\rho \to \infty$

Sending ρ to ∞, $\tanh^2(\rho)$ goes to 1, and, after using the product rule for the resulting $2gi\rho^2\partial_\rho\rho\phi^2$ term, this remains the only term.

$$\kappa\phi^1 = -\lambda\rho^2\phi^1 - \rho\partial_\rho\phi^1 - \rho^2\partial_\rho^2\phi^1 - 2gi\rho^2(\phi^2 + \rho\partial_\rho\phi^2)$$

Divide by ρ^2 and remove all disappearing terms:

$$\lambda\phi^1 + \partial_\rho^2\phi^1 + 2gi\rho\partial_\rho\phi^2 = 0$$

Only one term containing ρ is left:

$$2gi\rho\partial_\rho\phi^2 = 0$$

This results in the functions ϕ_∞^1 and ϕ_∞^2 being constants, which can be assumed to be symmetrical.

$$\Rightarrow \phi_\infty^2 = \phi_\infty^1 \to \text{const.}$$

Solving the symmetrical equations

With the behavior shown in 3.3, the coupled equations are assumed to be symmetrical, so the two functions ϕ_ρ^1 and ϕ_ρ^1 are rewritten as ϕ. The focus in this section lies on solving 33:

$$\phi\kappa + \lambda\rho^2\phi^1 + \rho\partial_\rho\rho\partial_\rho\phi + 2gi\rho^2 \tanh^2(\rho)\partial_\rho\rho\phi = 0 \tag{35}$$

The first attempt at solving 35 involved trying to find a standard integral solution for the equations, for which none could be found. The next was to rewrite the hyperbolic tangent portion as $\tanh^2(\rho) = \frac{\sinh^2(\rho)}{\cosh^2(\rho)}$, separate the quotient and try to solve the equation for the trigonometric functions expressed in terms of exponential functions. This did not work, as the sides of the differential equations had a difference in the power of ρ for all functions that were tried out, resulting in different numbers of peaks. While the absolute amplitudes of the additional peaks could be reduced to a certain extent, a quantitatively satisfactory solution could not be found. Thus, a series approximation was attempted.

Series approach

The aim is to use a power series approach to approximate the solution of the differential equation. This series would then be multiplied to a quickly decaying function such as $e^{-\rho^2}$ to ensure that it stays small for large ρ.

To avoid multiplying multiple infinite series arising from the term $\rho^2 \tanh \rho^2 \partial_\rho \phi_\rho^2$, the power series of $\tanh^2(\rho)$ up to the 10^{th} order is determined using the **Series**[] function in Wolfram Mathematica:

$$\tanh^2(\rho) \approx \rho^2 - \frac{2\rho^4}{3} + \frac{17\rho^6}{45} - \frac{62\rho^8}{315} + \frac{1382\rho^{10}}{14175} \equiv \rho^2 + a\rho^4 + b\rho^6 + c\rho^8 + d\rho^{10} \tag{36}$$

The individual terms are then written into series and brought to the same power ρ^n. While it is usually convenient to bring the sums to the same starting index, this is not possible for the terms from the expansion 36. In the following, the power series expressions for the individual terms of 35 are shown.

$$\kappa\phi = \kappa \cdot \sum_{n=0} a_n \rho^n$$

$$\lambda\rho^2\phi = \lambda \cdot \sum_{n=0} a_n \rho^{n+2} = \lambda \sum_{n=2} a_{n-2}\rho^n$$

$$\rho\partial_\rho\rho\partial_\rho\phi = \rho \cdot (\phi' + \rho\phi'') = \sum_{n=1} n a_n \rho^n + \sum_{n=2} n(n-1)a_n\rho^n$$

For the $\tanh^2(\rho)$ term, first the derivatives are rewritten, then the expansion 36 is multiplied to the sums.

$$2gi\tanh^2(\rho)\cdot\rho^2\partial_\rho\rho\phi = 2gi\tanh^2(\rho)\cdot\rho^2\cdot(\phi+\rho\phi') = 2gi\tanh^2(\rho)\cdot(\sum_{n=0} a_n\rho^{n+2} + \sum_{n=1} n a_n\rho^{n+2})$$

$$= 2gi\cdot[\sum_{n=0} a_n\cdot(\rho^{n+4} + a\rho^{n+6} + b\rho^{n+8} + c\rho^{n+10} + d\rho^{n+12}) +$$

$$+ \sum_{n=1} n a_n\cdot(\rho^{n+4} + a\rho^{n+6} + b\rho^{n+8} + c\rho^{n+10} + d\rho^{n+12})]$$

Next, the index shift is performed:

$$= 2gi\cdot[\sum_{n=4} a_{n-4}\rho^n + \sum_{n=6} a_{n-6}a\rho^n + \sum_{n=8} a_{n-8}b\rho^n + \sum_{n=10} a_{n-10}c\rho^n + \sum_{n=12} a_{n-12}d\rho^n +$$

$$+ \sum_{n=5}(n-4)a_{n-4}\rho^n + \sum_{n=7}(n-6)a_{n-6}a\rho^n + \sum_{n=9}(n-8)a_{n-8}b\rho^n + \sum_{n=11}(n-10)a_{n-10}c\rho^n + \sum_{n=13}(n-12)a_{n-12}d\rho^n]$$

These can now all be grouped together, and ρ^n can be factored out. This leads to the following power series, a part of which is expressed as products of sums for better legibility.

$$\kappa\cdot\sum_{n=0} a_n + \sum_{n=1} n a_n + \sum_{n=2}(\lambda a_{n-2} + n(n-1)a_n) + 2gi\cdot\left[\sum_{i\in\mathcal{I}}\sum_{n=i} b_{n,i} + \sum_{j\in\mathcal{J}}\sum_{n=j}(n-j+1)b_{n,i}\right] = 0 \tag{37}$$

The sets for the start indices are $\mathcal{I} = \{4,6,8,10,12\}$ and $\mathcal{J} = \{5,7,9,11,13\}$, and the relevant coefficients $b_{n,i}$ and $b_{n,j}$ are given in the following tables.

Table 1: Expressions for the coefficients $b_{n,i}$ and $b_{n,j}$.

i	j	$b_{n,i} = b_{n,j}$
4	5	a_{n-4}
6	7	$a_{n-6}a$
8	9	$a_{n-8}b$
10	11	$a_{n-10}c$
12	13	$a_{n-12}d$

One is now left with several power series which should be developed to the order $n = 13$ at the very least and were calculated by hand up to the order $n = 70$. The first few will be shown in the following tables, with a case distinction between the two κ values.

$\kappa = 0$

Because $\kappa = 0$, a_0 can be chosen as an arbitrary number. The following table shows the equations and resulting coefficients for the first terms:

Table 2: Coefficients a_n for the first few terms n of the series 37 for $\kappa = 0$.

n	Equation	a_n
0	$\kappa a_0 = 0$	a_0
1	$a_1 = 0$	0
2	$\lambda a_0 + 2a_2 + 2a_2 = 0$	$-\frac{\lambda}{4} \cdot a_0$
3	$\lambda a_1 + 3a_3 + 6a_3 = 0$	0
4	$\lambda a_2 + 4a_4 + 12a_4 + 2gia_0 = 0$	$-\frac{1}{16} \cdot (\lambda a_2 + 2gia_0)$

One can see, whether by calculating the terms or looking at the sums, that the a_n disappear for odd n.

$\kappa = -1$

Now, a_1 can be chosen arbitrarily, and one gets the opposite situation of 2 - the a_n disappear for even n. The results for the first terms are shown in the following table:

Table 3: Coefficients a_n for the first few terms n of the series 37 for $\kappa = -1$.

n	Equation	a_n
0	$\kappa a_0 = 0$	0
1	$-(\kappa + 1)a_1 = 0$	a_1
2	$\lambda a_0 + (\kappa + 4)a_2 = 0$	0
3	$\lambda a_1 + (\kappa + 9)a_3 = 0$	$\frac{-\lambda a_1}{10}$
4	$\lambda a_2 + (\kappa - 16)a_4 = 0$	0
5	$\lambda a_3 + 24a_5 + 4gia_1 = 0$	$-\frac{1}{24}(\lambda a_3 + 2gi \cdot 2a_1)$

(Cont.) Remark: Angular component

From 32, it is apparent from the series coefficients that the values of ω for which the function is not zero everywhere are the following:

$$-\omega^2 = \kappa$$
$$\Rightarrow \omega = \begin{cases} 0 & \kappa = 0 \\ \pm 1 & \kappa = -1 \end{cases} \tag{38}$$

4 Results

4.1 Function convergence

For both possible values of κ, the function behavior is observed at increasing orders of the sum (here: up to the 70^{th} order). While the polynomials diverge, the points at which they diverge are of importance - if the function stays more stable for higher orders before divergence, this is evidence of the polynomial being a possible candidate for a solution of the differential equation.

The following plots show the divergence of the eigenfunction series $f(\rho)$ at the three highest calculated orders n. Only even orders are shown because for the others, the function is equal to zero for $\kappa = 0$ - the analogous goes for the odd orders in the case of $\kappa = -1$. For purposes of consistency, the eigenvalue for all series is chosen to be $\lambda = 1$ in this section.

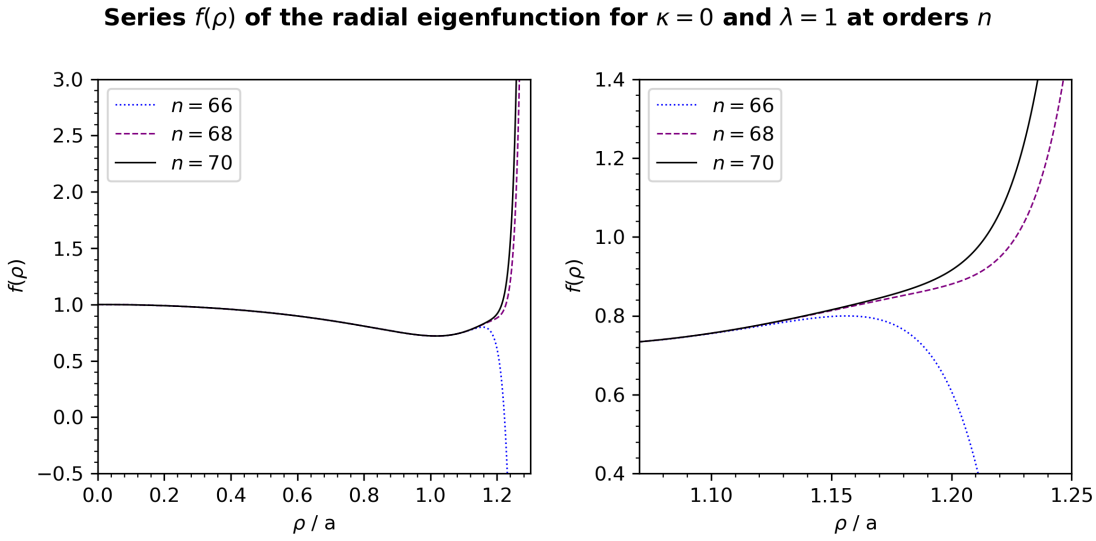

Figure 2: Shown above are the series $f(\rho)$ at the orders $n = 66$, $n = 68$ and $n = 70$ for $\kappa = 0$. The left plot shows the full domain from $\rho = 0$ up to the point of divergence, and the right plot zooms in on the exact points of divergence.

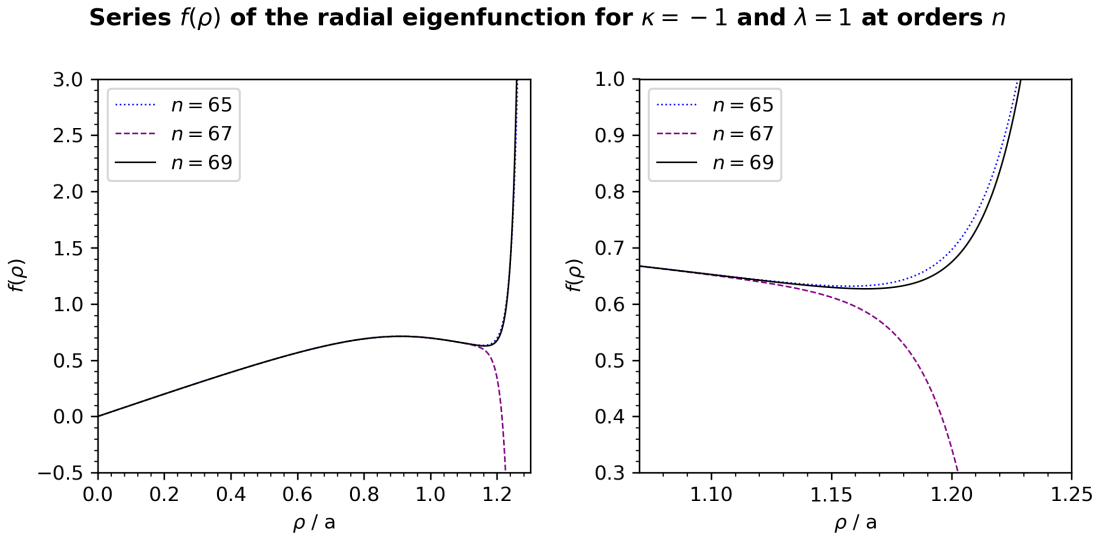

Figure 3: Shown above are the series $f(\rho)$ at the orders $n = 65$, $n = 67$ and $n = 69$ for $\kappa = -1$. The left plot shows the full domain from $\rho = 0$ up to the point of divergence, and the right plot zooms in on the exact points of divergence.

It is apparent from 2 and 3 that the series converges into a function at higher and higher orders with the lower orders diverging first. As powers with different signs for the coefficients dominate the expression, the divergence alternates between $-\infty$ and $+\infty$, however, there is no clear pattern here.

For the two values of κ, the series have similar convergence behaviors and the second to last series orders ($n = 68$, $n = 67$) branch off between 1.10 a and 1.15 a, i.e. in the same order of magnitude. For $\kappa = -1$, the function diverges slightly more quickly.

The following figure shows the comparison between the sides of the differential equation 35 applied to the series $f(\rho)$. For clearer axis labels in the plot, the expression will be rewritten as an operator:

$$(\kappa + \rho\partial_\rho\rho\partial_\rho + 2gi\rho^2\tanh^2(\rho) + \lambda\rho^2)f(\rho) \equiv D_\rho$$

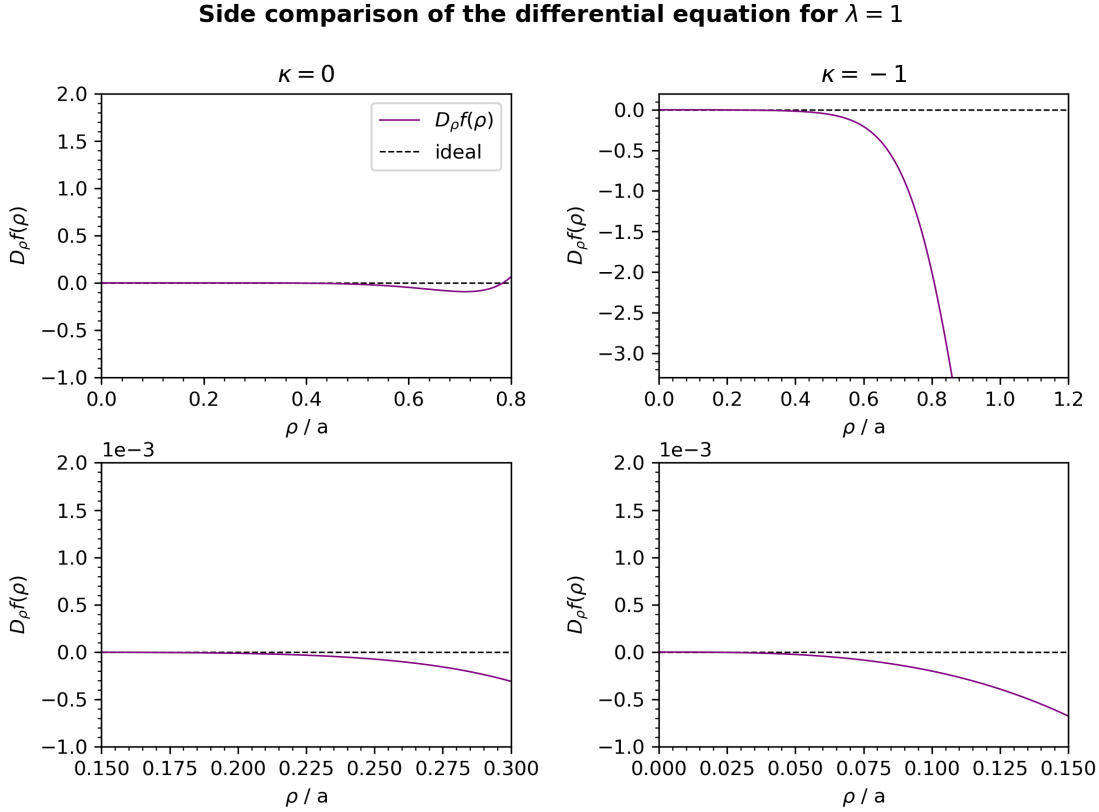

Figure 4: The plots pictured above show the differential equation 35 applied to the series $f(\rho)$ in the form of $D_\rho f(\rho)$ for the two possible κ values (left: $\kappa = 0$, right: $\kappa = -1$). The top plots show the full domains until divergence and the bottom ones zoom into the points at which the expression stops corresponding "exactly" to zero. Ideally, the expression should stay at zero for as long as possible.

There is a significant difference in divergence speed between the two κ values, with the ρ value at which the function for $\kappa = -1$ diverges being about an order of magnitude smaller than that for $\kappa = 0$. This difference could be attributed to the higher order (70) or the first polynomial, but due to the fact that it is only a difference of one order, this can be neglected. It is more likely that the odd polynomials contain more fluctuations and therefore deviate from 0 at lower values of ρ.

4.2 Examining a few eigenvalues

The following plots, like 4, show the comparison of the two sides of the equation. Here, the eigenvalues are varied for a small range $\lambda \in \{-10, -5, -1, 0, 1, 5, 10\}$. For easier visualization, the values for $\lambda \leqslant 0$ are plotted in the first figure, and the values for $\lambda > 0$ in the second.

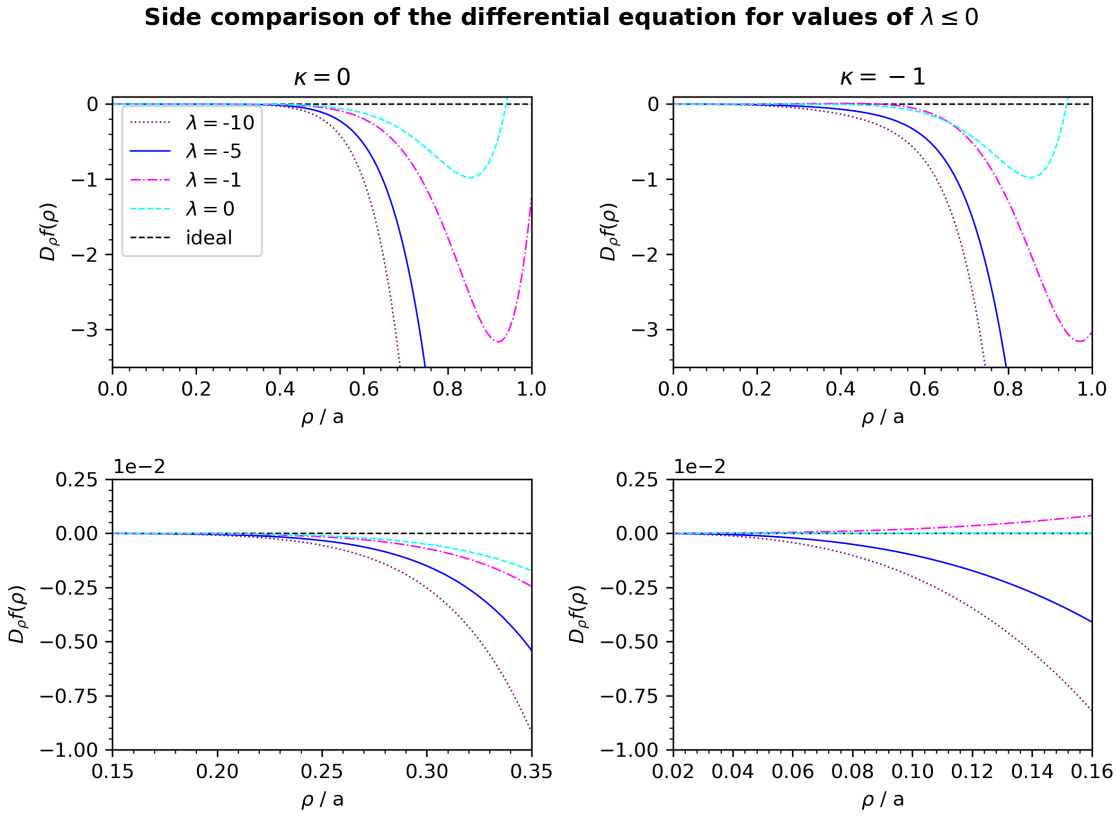

Figure 5: The plots pictured above show the differential equation 35 applied to the series $f(\rho)$ in the form of $D_\rho f(\rho)$ for various values of λ and the two possible κ values (left: $\kappa = 0$, right: $\kappa = -1$). The top plots show the full domains until divergence and the bottom ones zoom into the relevant divergence points.

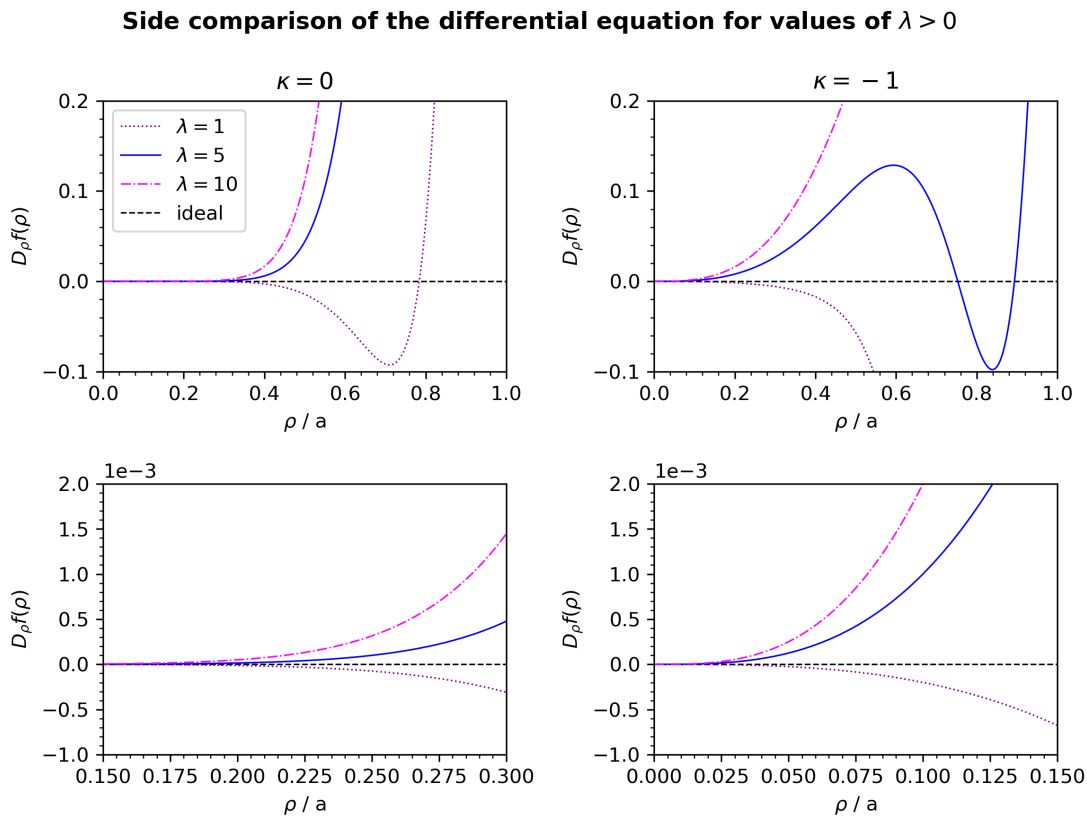

Figure 6: The plots pictured above show the differential equation 35 applied to the series $f(\rho)$ in the form of $D_\rho f(\rho)$ for various values of λ and the two possible κ values (left: $\kappa = 0$, right: $\kappa = -1$). The top plots show the full domains until divergence and the bottom ones zoom into the relevant divergence points.

From the plots 5 and 6 it is apparent that while there is a degree of convergence for all displayed eigenvalues, those with a smaller absolute value have better convergence. For $\lambda = 0$, the behavior is the most stable while the larger eigenvalues diverge more and more quickly. This is likely due to the quadratic term $\lambda\rho^2$ multiplied to the polynomial $f(\rho)$, which simply causes a larger polynomial. Despite this, all λ tested out in this small range show some convergence at low ρ, implying that the spectrum could contain both positive and negative eigenvalues.

The difference between the divergences of the two κ values seen in 4.1 appears to be consistent for the other eigenvalues. The polynomial for $\kappa = -1$ diverges about an order of magnitude more quickly than that for $\kappa = 0$.

4.3 Limitations

Several simplifications that were made for the calculation process are worth noting. The results currently apply to two-dimensional polar coordinates, and still need to be extended into the four-dimensional space. Additionally, the current eigenfunction is shown for real numbers and an analytical continuation would be necessary to include the imaginary portion of 29.

It is also assumed that the solutions to the coupled equations 24 and 25 are completely symmetric. Although the limit behaviors examined in 3.3 are the same, the functions do not necessarily need to behave the same way between these limits.

5 Summary and Outlook

The eigenvalue equation of the Faddeev-Popov operator for the potential configuration $\tanh^2(x)$, simplified to the two-dimensional case and then coordinate-transformed to polar coordinates, was split up by color, leading to three differential equations, two of which were coupled. The coupled equations were separated into radial and angular components. Assuming symmetry between the coupled equations, the radial portion of the equation was then approximated by a series approach:

$$\kappa \cdot \sum_{n=0} a_n + \sum_{n=1} n a_n + \sum_{n=2} (\lambda a_{n-2} + n(n-1)a_n) + 2gi \cdot \left[\sum_{i \in \mathcal{I}} \sum_{n=i} b_{n,i} + \sum_{j \in \mathcal{J}} \sum_{n=j} (n-j+1) b_{n,i} \right] = 0$$

for the sets $\mathcal{I} = \{4, 6, 8, 10, 12\}$ and $\mathcal{J} = \{5, 7, 9, 11, 13\}$.

Depending on the results of the angular component (either $\omega = 0$ or $\omega = \pm 1$), two possible series emerged. These were calculated up to the 70^{th} order and then examined for convergence. The influence of positive and negative eigenvalues were examined as well for a small range of $\lambda \in \{-10, -5, -1, 0, 1, 5, 10\}$. The functions appear to converge for higher and higher orders of the series, and fulfill the differential equation for small values of ρ.

To verify the series as solutions to the differential equation, it would be necessary to include the generalizations mentioned in 4.3, as well as calculating significantly higher orders of the series to check convergence at larger values of ρ.
Should the solution be verified, it appears promising that negative eigenvalues such as the ones shown in 4.2 could satisfy the eigenvalue equation, implying that the potential configuration could be a possible candidate for going beyond the first Gribov region.

I would like to express my special thanks to Felix Halbwedl for assisting in the formatting of this thesis.

References

[1] David J. Griffiths. *Introduction to Electrodynamics*. Cambridge University Pr., June 2017. ISBN: 1108420419. URL: https://www.ebook.de/de/product/29245261/david_j_griffiths_introduction_to_electrodynamics.html.

[2] Allen Hatcher. *Algebraic Topology*. Cambridge University Pr., Dec. 2001. ISBN: 0521795400. URL: https://www.ebook.de/de/product/3255852/allen_hatcher_algebraic_topology.html.

[3] Axel Maas. "On the spectrum of the Faddeev-Popov operator in topological background fields". In: *Eur.Phys.J.C48:179-192,2006* (Nov. 2005). DOI: 10.1140/epjc/s10052-006-0003-y. arXiv: hep-th/0511307 [hep-th].

[4] Daniel V. Schroeder Michael E. Peskin. *An Introduction To Quantum Field Theory*. Taylor and Francis Inc, Oct. 1995. 866 pp. ISBN: 0201503972. URL: https://www.ebook.de/de/product/3595300/michael_e_peskin_daniel_v_schroeder_an_introduction_to_quantum_field_theory.html.

[5] Rowland. *Fibre Bundle*. Wolfram Mathworld. URL: https://mathworld.wolfram.com/FiberBundle.html.

[6] Lewis H. Ryder. *Quantum Field Theory*. Cambridge University Press, Mar. 2016. 508 pp. ISBN: 0521478146. URL: https://www.ebook.de/de/product/3238955/lewis_h_ryder_quantum_field_theory.html.

[7] I. M. Singer. "Some remarks on the Gribov ambiguity". In: *Communications in Mathematical Physics* 60.1 (Feb. 1978), pp. 7–12. DOI: 10.1007/bf01609471.

[8] Eric W. Weissstein. *Helmholtz Differential Equation - Polar coordinates*. Wolfram Mathworld. URL: https://mathworld.wolfram.com/HelmholtzDifferentialEquationPolarCoordinates.html.